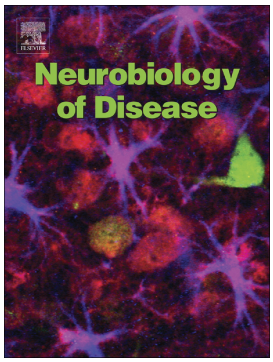

Synapsin I phosphorylation is dysregulated by beta-amyloid oligomers and restored by valproic acid

Jade Marsh, Saifuddien Haji Bagol, Robin S.B. Williams, George Dickson, Pavlos Alifragis

PII: S0969-9961(17)30137-7
DOI: doi: 10.1016/j.nbd.2017.06.011
Reference: YNBDI 3981

To appear in: *Neurobiology of Disease*

Received date: 25 November 2016
Revised date: 2 June 2017
Accepted date: 20 June 2017

Please cite this article as: Jade Marsh, Saifuddien Haji Bagol, Robin S.B. Williams, George Dickson, Pavlos Alifragis , Synapsin I phosphorylation is dysregulated by beta-amyloid oligomers and restored by valproic acid, *Neurobiology of Disease* (2017), doi: 10.1016/j.nbd.2017.06.011

Synapsin I phosphorylation is dysregulated by beta-amyloid oligomers and restored by valproic acid

Jade Marsh, Saifuddien Haji Bagol[1], Robin SB Williams, George Dickson, Pavlos Alifragis*
Centre for Biomedical Sciences, School of Biological Sciences, Royal Holloway University of London, Egham, Surrey, TW20 0EX, UK
[1]Current address Tungkulikn Highway, Kg Gadong, BE 3719, Brunei, Darussalam
* Corresponding author. Email: pavlos.alifragis@rhul.ac.uk

Abstract

Alzheimer's disease is the most prevalent form of dementia in the elderly but the precise causal mechanisms are still not fully understood. Growing evidence supports a significant role for Aβ42 oligomers in the development and progression of Alzheimer's. For example, intracellular soluble Aβ oligomers are thought to contribute to the early synaptic dysfunction associated with Alzheimer's disease, but the molecular mechanisms underlying this effect are still unclear. Here, we identify a novel mechanism that contributes to our understanding of the reported synaptic dysfunction. Using primary rat hippocampal neurons exposed for a short period of time to Aβ42 oligomers, we show a disruption in the activity-dependent phosphorylation cycle of SynapsinI at Ser9. SynapsinI is a pre-synaptic protein that responds to neuronal activity and regulates the availability of synaptic vesicles to participate in neurotransmitter release. Phosphorylation of SynapsinI at Ser9, modulates its distribution and interaction with synaptic vesicles. Our results show that in neurons exposed to Aβ42 oligomers, the levels of phosphorylated Ser9 of SynapsinI remain elevated during the recovery period following neuronal activity. We then investigated if this effect could be targeted by a putative therapeutic regime using valproic acid (a short branch-chained fatty acid) that has been proposed as a treatment for Alzheimer's disease. Exposure of Aβ42 treated neurons to valproic acid, showed that it restores the physiological regulation of SynapsinI after depolarisation. Our data provide a new insight on Aβ42-mediated pathology in Alzheimer's disease and supports the use of Valproic acid as a possible pharmaceutical intervention for the treatment of Alzheimer's disease.

Highlights

- Activity dependent availability of synaptic vesicles is enhanced by Aβ42 oligomers
- Aβ42 oligomers reduce the recovery of SnpI after neuronal activity
- VPA reverses the effects of Aβ42 oligomers on SnpI

Key Words

Alzheimer's, Aβ42, Synaptic vesicles, neuronal activation, Synapsin, VPA

Introduction

Alzheimer's disease (AD) is a progressive neurodegenerative disorder, characterised by synaptic dysfunction and neuronal loss. The phenotypical hallmarks of the disease are intracellular neurofibrillary tangles (NFT) consisting of aggregates of hyperphosphorylated tau protein and extracellular deposits (amyloid plaques) comprising amyloid-beta (Aβ) peptides. Aβ peptides are hydrophobic and readily oligomerise and aggregate, forming fibrillar structures deposited in extracellular plaques. It is currently believed that early synaptic dysfunction of excitatory synapses underlying memory impairment during the early stages of the disease is induced by soluble oligomeric forms of Aβ42 (Aβ42O) and precedes plaque formation (Hsia et al., 1999; Lacor et al., 2007; Lambert et al., 1998; Oddo et al., 2003; Oddo et al., 2006; Shankar et al., 2007; Shrestha et al., 2006; Walsh et al., 2002; Wang et al., 2002). Exposure of neurons to Aβ42O induces a multitude of synaptic defects such as a decrease in excitatory post synaptic potentials (EPSPs) and inhibition of NMDAR-dependent LTP. These defects have been associated with increased amounts of glutamate at the synaptic cleft, either through the reduction of glutamate uptake, or by enhanced glutamate release. Consequently, excitotoxicity, desensitisation of the glutamate receptors and inhibition of LTP is induced (Abramov et al., 2009; Arias et al., 1995; Harris et al., 1995; Kabogo et al., 2008; Li et al., 2009; Li et al., 2011; Puzzo et al., 2008).

Recent studies suggest that intracellular Aβ42 (iAβ42) induces presynaptic defects by interfering with neurotransmitter (NT) release (Abramov et al., 2009; Billings et al., 2005; Kelly and Ferreira, 2007; Oddo et al., 2003; Oddo et al., 2006; Park et al., 2013; Parodi et al., 2010; Ripoli et al., 2014; Russell et al., 2012). It has been shown that iAβ42 induces depletion of synaptic vesicles (SV) in a time and concentration dependent manner (Parodi et al., 2010) and affect the relative size of different SV pools (Park et al., 2013). Although several effects of Aβ peptides on SV dynamics have been described, how these effects arise is still not fully understood. Recently, we reported that a contributing factor to presynaptic defects could be the disruption of the interaction between two SV proteins, Synaptophysin (Syp) and Synaptobrevin by Aβ42O (Russell et al., 2012). Here, we provide evidence of an additional mechanism by which Aβ42O can modulate the availability of SVs. Our results suggest that in neurons exposed to Aβ42O, the phosphorylation dynamics of SynapsinI (SnpI) is changed. SnpI belongs to a family of pre-synaptic phosphoproteins that are essential components of synaptic fine-tuning and remodelling. They organise the pools of SVs during neuronal activity through direct association/dissociation cycles, acting as key regulators of the availability of SVs to participate in neurotransmitter (NT) release (Cesca et al., 2010). It has been suggested that Snps serve as adaptor proteins that tether SVs to an actin mesh under resting conditions by binding to SVs as well as the actin cytoskeleton and clustering them in the resting pool (Cesca et al., 2010; Orenbuch et al., 2012). However, activity-dependent phosphorylation/dephosphorylation cycles at key residues of Snps induce transient disassembly of Snps from the SVs (Jovanovic et al., 2001). Consequently, SVs are released from the resting pool, enabling their participation in neurotransmitter release whilst Snps diffuse in the axon (Shupliakov et al., 2011) but readily re-cluster after the cessation of synaptic activity (Chi et al., 2001; Hosaka et al., 1999). Ser9 (site1) is within a small N-terminal lipid-binding domain that upon synaptic activity, gets phosphorylated, leading to dissociation from SVs (Hosaka et al., 1999). Under physiological conditions, activity-dependent increases in $pSnpI^{Ser9}$ levels enhance neurotransmitter release (Benfenati et al., 1989; Benfenati et al., 1992; Benfenati et al., 1991). Interestingly, the levels of phosphorylated SnpI at position 1 (Ser9) are enhanced in AD post-mortem tissues (Parks et al., 1991).

Here we explore the hypothesis that exposure of neurons to Aβ42O has a direct impact on the levels of SnpI phosphorylation. Double immunolabeling in primary rat hippocampal neurons was performed for SnpI or $pSnpI^{Ser9}$ and Synaptophysin (Syp), a synaptic vesicle associated protein that labels pre-synaptic boutons. Quantification of the extent of overlap between Syp and SnpI or $pSnp^{Ser9}$, showed that although Aβ42O do not interfere with the dispersion pattern of SnpI during neuronal activity, they deregulate the phosphorylation/dephosphorylation cycle of $pSnp^{Ser9}$. In addition, we examined available drugs that could reverse this effect. Valproic Acid (VPA), a short branched chain

fatty acid, is a commonly used drug for treatment of epilepsy and bipolar disorder and based on evidence from mouse models, has also been proposed to be beneficial at early stages of AD (Park et al., 2014; Qing et al., 2008). VPA has been found to affect LTP and LTD and combat various aspects of AD-related pathology (Chang et al., 2010; Hu et al., 2011; Leng et al., 2008; Qing et al., 2008; Williams and Bate, 2016; Zhang et al., 2003). Since VPA has also been shown to prevent Aβ42 induced reduction in SV recycling (Williams and Bate, 2016) and to induce clustering of SnpI in developing neurons (Hall et al., 2002), we examined if it could be used to reduce the effects of Aβ42O in the regulation of SnpI. Our results show that indeed, VPA can abrogate the effects of Aβ42O on the dynamics of SnpI regulation in a concentration dependent manner.

Materials and Methods

Primary hippocampal neuronal cultures.

All animal experiments were performed according to Home Office regulations in compliance with the Animals Scientific Act 1986. Primary cultures of CA3-CA1 hippocampal neurons were prepared from E18 Sprague Dawley rat embryos as previously described (Russell et al., 2012)[OBJ]. Briefly, cells were plated at a density of either 75,000 or 500,000 cells on poly-D-lysine (Sigma, 0.1mg/ml in borate buffer pH 8.5) coated glass cover slips or 6-well plates respectively. The plating medium was DMEM supplemented with 5% FBS, penicillin/streptomycin (P/S) and 0.5mM l-glutamine (all from Invitrogen). On the next day the medium was changed to full Neurobasal medium (Neurobasal medium supplemented with B27, P/S, 0.5mM l-glutamine, all from Invitrogen). Cultures were incubated at 37^{o}C and 5% CO_2, and were used routinely between 18 to 21 DIV. Immuno labelling for vGlut (Synaptic Systems) and Gad65 (Chemicon) was performed to ensure our cultures were enriched in glutamatergic neurons (Sup Fig 1)

Preparation of AβO and neuronal treatment

Preparation of Aβ peptides and treatment of neurons to study the effects of iAβ42 has been previously described (Russell et al., 2012). Briefly, Aβ42 (American peptides) was prepared by dissolving the peptide in DMSO (1mM). The reconstituted peptides were diluted in PBS at a working concentration of 300µM and stored in aliquots at -80°C. Peptides were diluted in working concentration in full Neurobasal medium immediately after thawing and were not frozen again. Since reconstituted Aβ42 peptides rapidly aggregate to form oligomers, protofibrils and fibrils, we routinely examined the aggregation state of our peptides on native and SDS polyacrylamide gels. On native gels, we observed a predominant band with a molecular weight of ~20 kDa (Sup Fig 2A) indicating that our peptide preparation consists of small oligomers believed to be the toxic species (Selkoe, 2012). These oligomers could be broken down to monomers (4.5 kD) - trimers (13.5 kD) on an SDS PAGE gel (Sup Fig 2B) suggesting that they had not adopted a β-sheet conformation.

To ensure the observed effects were produced by intracellular Aβ42, neurons were treated exactly as previously described (Russell et al., 2012). Briefly, neurons were incubated with Aβ42O (diluted in full Neurobasal medium at 300nM final concentration) for 30min. Aβ42O were removed by replacing the medium with fresh full Neurobasal medium with or without drugs (for consistency medium in control neurons was also replaced) and the cells were left to recover for 2hrs. Immunolabelling of primary neurons for Aβ42 (6E10 Ab from Covance) and GluN2A/B ((Chemicon) confirmed our previous data and showed Aβ42Os present at the presynaptic compartment of glutamatergic synapses (Sup Fig 3). Synchronisation of neurons was performed after the 2hr recovery period by replacing the medium with a salt solution containing KCl (70mM KCl, 44mM NaCl, 2mM $CaCl_2$, $MgCl_2$, 20mM HEPES and 30mM glucose) for 5min. Recovery of neurons from neuronal activity involved washing the cells and incubation for a further 15mins at 37^{o}C and 5% CO_2 in fresh full Neurobasal medium.

Immunocytochemistry

Following treatment, coverslips were rinsed once with pre-warmed (37^{0}C) PBS and fixed with 4% paraformaldehyde (PFA), 2% Sucrose in PBS. Fixed neurons were washed with TBS, permeabilised with

0.1% Tween-20 and 5% horse serum in TBS for 45min at room temperature, and incubated with primary antibodies overnight at 4°C. Coverslips were incubated with different combinations of primary and secondary antibodies and then mounted using the ProLong Gold reagent (InvitrogenUK). The primary antibodies used were combinations of: a rabbit anti-Syp antibody (Santa Cruz, sc-7568) and a mouse anti-Snp antibody (Santa Cruz, sc-37662); or a mouse anti-Syp (Sigma UK, S5768) and a Rabbit anti- $pSnp^{Ser9}$ antibody (Abcam, ab76260). Fluorescent secondary antibodies were all from Invitrogen: anti-rabbit Alexa Fluor 568; anti-mouse Alexa Fluor 488; anti-mouse Alexa Fluor 647. The cells were visualised on a spin disc confocal system (CARV from Digital Imaging Solutions) with an EM-CCD camera (Rolera/QI Cam 3500) mounted on an Olympus X71 microscope, using a 100x fluoplan objective (NA 4.2). The microscope confocal system was supported by Image Pro 6.0 software.

Image analysis

The image analysis was performed as previously described (Semerdjieva et al., 2013). Briefly, 10-15 images (from a minimum of three independent experiments) were analysed using the JaCoP plugin for ImageJ (Bolte and Cordelieres, 2006), to calculate the split Mander's coefficient. For consistency, the background of each image was removed by selecting two random areas devoid of staining within the images, the intensity was measured on each channel independently using ImageJ and the average background measurement was removed from the entire single channel image before analysis. No threshold was applied to avoid introducing a non-consistent bias to our calculations. To avoid potential digital overlap, all images were single section confocal images.

Western blotting

Proteins were extracted in 20mM HEPES pH7.5, 1mM EDTA, 150mM NaCl, 1% NP-40 and 1mM dithiothreitol supplemented with protease (Roche) and phosphatase (Thermo Scientific) inhibitor cocktails. The protein concentration of the protein extract was determined by Bradford's Protein Assay. 15µg of total protein were separated on 12% Tris-Glycine gels at 120V and transferred to nitrocellulose membrane at 10V for 16 hours in transfer buffer (200mM Glycine, 25mM Tris Base, 20% Methanol). Blots were blocked with 2.5% non-fat dry milk in Tris-buffered saline (50mM Tris Base, 150mM NaCl) containing 0.05% Tween-20, pH 7.5, for 1hr and 30mins with agitation. Following this, blots were incubated at room temperature for 2 hours with primary antibodies and for 1 hour with secondary antibodies diluted in 2.5% non-fat dry milk. Detection of proteins was performed using the Odyssey® imaging scanner (LI-COR Biosciences). Primary antibodies used were a mouse anti-Syp IgM antibody (Novus Biologicals, NBP1-97459); a mouse anti-Snp antibody (Santa Cruz, sc-37662); a rabbit anti-Snp pSer9 antibody (Novus Biologicals, NB300-180), a mouse anti-actin antibody (SIGMA A5316), a mouse anti-Aβ (clone 6E10) and a Rabbit p-PP2A(Tyr 307)-Calpha/beta (Santa Cruz, sc-12615-R). Fluorescent secondary antibodies used were a goat anti-mouse 680 (NEB, 5470S) and a goat anti-rabbit 800 (NEB, 5151S).

Statistical analysis

All data in this study are reported as mean ± SEM. Statistical analysis of data was performed by a one-way ANOVA followed by a Tukey's multiple comparisons test using the XLSTAT add-in for Excel, or by a student's T-Test. Overall p-values are presented in tables in the supplementary data. Only significant p-values are discussed in the manuscript.

Results

Effect of Aβ42O on the activity-dependent dispersal of SnpI

We have previously reported that a brief exposure of neurons to nanomolar concentrations of Aβ42O followed by a recovery period results in its internalisation and its presence at the presynaptic compartment, where it disrupts the interaction between Syp and VAMP2 (Russell et al., 2012). To investigate the effects of internalised Aβ42O on the regulation of SnpI we adopted a similar approach. Mature hippocampal neurons were cultured for 18-21 days *in vitro* to provide well-established synaptic junctions. Double immunolabeling for SnpI and Syp was performed in fixed neurons to visualise how the distribution of SnpI at synapses was altered during neuronal activity following Aβ42O treatment in relation to Syp, a synaptic vesicle marker. Initially, we compared the co-localisation of SnpI and Syp in non-synchronised cultures between control neurons and neurons exposed to Aβ42O for 30 min followed by a 2hr recovery in culture medium. In these experiments, SnpI and Syp showed extensive co-localisation in pre-synaptic boutons in the absence or presence of Aβ42O (Fig 1A and D respectively). To quantify the dynamic of this distribution, we calculated the extent of overlap between SnpI over Syp (expressed by the Mander's co-efficient value) as previously described (Semerdjieva et al., 2013). Our results showed that SnpI overlapped extensively with Syp in both untreated and Aβ42O-treated neurons. No difference was found between control and Aβ42O treated neurons (Fig 1G, black bars), suggesting that Aβ42O did not affect the diffusion of SnpI from synaptic contacts under resting conditions.

Since neurons in culture fire asynchronously, we hypothesised that an effect of Aβ42O in the activity-dependent dispersal of SnpI might be difficult to observe under basal conditions. Thus, we repeated our experiment in synchronised cultures. Depolarisation of neurons by exposure to KCl for 5min prior to fixation induced a reduction in the localisation of SnpI at Syp-labelled synaptic contacts (Fig 1B and grey bar in G, with $p<0.0001$ compared to non-depolarised control neurons) indicating that neuronal activity resulted in dispersion of SnpI from pre-synaptic boutons. A similar change in the distribution of SnpI was also observed in neurons exposed to Aβ42O following depolarisation (Fig 1E and grey bar in G, with $p<0.0001$ compared to non-depolarised Aβ42O treated neurons).

Finally, double immunolabeling for SnpI and Syp in neurons allowed to recover for 15 min after depolarisation, showed that the co-localisation between the two proteins in both untreated and Aβ42O treated neurons was re-established (Fig 1C, F and white bars in G with $p<0.0001$ compared to depolarised neurons). These results confirm previously published data regarding the dynamics of the activity-dependent dispersal and re-clustering of SnpI (Chi et al., 2001). In addition, these observations indicate that acute exposure of primary neurons to Aβ42O has no effect on the dispersal of SnpI.

Effect of Aβ42 oligomers on activity-dependent phosphorylation of SnpI

Since our data suggest that Aβ42O do not affect the activity-dependent distribution of SnpI, we then investigated if Aβ42O had an effect on its regulation by focusing on the phosphorylation of Ser9. To do so, we examined its distribution by double immunolabeling for $pSnpI^{Ser9}$ and Syp in neurons treated under the same experimental conditions described earlier. In non-synchronised neurons, co-localization of $pSnp^{Ser9}$ with Syp at pre-synaptic contacts was similar between control and Aβ42O treated neurons (Fig 2A, D and black bars in G), although this was not as pronounced as SnpI/Syp co-localisation. This suggests that under basal conditions, only a fraction of synapses were activated and that exposure of neurons to Aβ42O had no detectable effect in the presence of $pSnpI^{Ser9}$ at synaptic contacts.

Next, we examined the effect of Aβ42O on the distribution of $pSnp^{Ser9}$ at synaptic contacts of synchronised neurons. Double immunolabeling for $pSnpI^{Ser9}$ and Syp, showed an overall increase of $pSnpI^{Ser9}$ at synaptic boutons, compared to asynchronously firing synapses, both in the presence or absence of Aβ42O (Fig 2B, E and grey bars in G, with $p<0.0001$ compared to non-synchronised neurons) suggesting that depolarisation of neurons increases the presence of $pSnpI^{Ser9}$ at synaptic contacts and that Aβ42O treatment does not affect this increase.

Finally, in neurons recovered for 15 min post-synchronisation, we observed a significant reduction of $pSnpI^{Ser9}$ labelling at synaptic contacts in control neurons, whereas labelling of $pSnpI^{Ser9}$in

Aβ42O treated neurons remained pronounced (Fig 2 C, F). Quantification of the extent of overlap between Syp and pSnpI^{Ser9} in those conditions showed that even though the expected reduction of pSnpI^{Ser9} at synaptic boutons was observed in control neurons as well as in Aβ42O-treated neurons 15 min after depolarisation ($p<0.0001$ for control neurons and $p=0.048$ for neurons exposed to Aβ42O), a significant difference in the presence of pSnpI^{Ser9} between control and Aβ42O treated neurons was evident (Fig 2G white bars, with $p<0.0001$ between control neurons and Aβ42O treated neurons).

Collectively, our data show that in neurons exposed to Aβ42O, the diffusion of SnpI upon depolarisation and its subsequent re-clustering at synaptic contacts recovering from neuronal activity is not affected. Interestingly however, although the levels of pSnpI^{Ser9} at synaptic contacts in control and in Aβ42O treated neurons remain similar during the activation period, during the recovery period the levels of pSnpI^{Ser9} at synaptic contacts remain high in Aβ42O exposed neurons. This suggests that even though SnpI re-clusters following neuronal activity in neurons exposed to Aβ42O, its ability to interact with SVs is abrogated during that period.

Effects of VPA on the dynamics of SnpI regulation in neuronal cultures

Our results so far suggest that Aβ42O affect the activity-dependent dynamics of the phosphorylation/dephosphorylation cycle of SnpI at Ser9. Since SnpI has an essential role in modulating SV dynamics and is likely to have an impact on neurotransmitter release, we next investigated if this effect could be reversed by potential therapeutic drugs.

VPA has been previously reported to affect SnpI clustering in neurons (Hall et al., 2002) , hence we examined the effect of VPA on SnpI distribution under our experimental conditions. In these experiments, neurons were acutely treated with 10mM VPA for 2 hours after the removal of Aβ42O from the medium.

First, we investigated the effect of VPA alone on SnpI distribution. In non-synchronised neurons, double immunolabeling for SnpI and Syp in control and VPA-treated neurons revealed no alteration in the dispersal of SnpI in synaptic boutons (Fig 3A, D and black bars in G). In synchronised neurons, equivalent VPA treatment caused a small but statistically significant increase of SnpI at synapses (Fig 3B, E and grey bars in G, with $p=0.03$ between control neurons and VPA treated neurons,), suggesting that VPA restricts the activity-dependent dispersal of SnpI. Finally, we examined the effect of VPA on the re-clustering of SnpI in neurons recovered for 15 minutes after synchronisation. Our data showed that VPA treatment had no effect on SnpI re-clustering following recovery from neuronal activity (Fig 3 C, F and white bars in G). These results confirm an earlier study (Hall et al., 2002) and in addition, show that VPA restricts the activity-dependent dispersal of SnpI in mature primary neurons.

Next we examined the effect of VPA on pSnpI^{Ser9}. In non-synchronised neurons, double immunolabeling for Syp and pSnpI^{Ser9} showed slightly elevated levels of pSnpI^{Ser9} at synaptic contacts in VPA-treated neurons compared to control neurons (Fig 4 A, D and black bars in G, with $p=0.026$ between control neurons and VPA treated neurons) indicating that acute treatment of primary neurons with VPA marginally restricts the activity-dependent dispersal of pSnpI^{Ser9}. In synchronised neurons, VPA treatment did not alter pSnpI^{Ser9} distribution (Fig 4 B, E), as confirmed by quantification of pSnpI^{Ser9} to Syp overlap (Fig 4 G, grey bars). Similarly, VPA treatment did not alter the distribution of pSnpI^{Ser9} at synaptic contacts of neurons recovered for 15 min after depolarisation as confirmed by our calculations (Fig 4 C, F and white bars in G). These results suggest that VPA has a limited effect on the distribution of pSnpI^{Ser9}.

VPA reverses the effects of Aβ42 oligomers on pSnpI^{Ser9}

We next examined if co-treatment of neurons with VPA affects the Aβ42O induced increase of pSnpI^{Ser9} at the presynapse. To ensure that the internalisation of Aβ42O was not affected, we incubated neurons with VPA after removal of Aβ42O containing culture medium. In these experiments the localisation of pSnpI^{Ser9} at synaptic contacts was assessed in control and in Aβ42O treated neurons as previously described and was compared to neurons exposed to Aβ42O for 30 min followed by incubation with medium containing VPA. We initially carried this out in neurons recovering from

neuronal activity. Double immunolabeling for pSnpI^{Ser9} and Syp showed a reduction of pSnpI^{Ser9} at the presynapse in recovering Aβ42O/VPA treated neurons compared to Aβ42O treated neurons recovering in medium without VPA (Fig 5 A-C). Quantification of the extent of overlap between Syp and pSnpI^{Ser9} confirmed our observation (Fig 5 D, $p<0.0001$ compared to Aβ42O treated neurons). These results suggest that VPA inhibits Aβ42O from inducing elevated levels of pSnpI^{Ser9} at synaptic contacts in mature primary rodent neurons.

Finally, to show that co-treatment of neurons with Aβ42O and VPA had no additive effect, we examined if the combined exposure of Aβ42O and VPA in non-synchronised and synchronised neurons affected the distribution of pSnpI^{Ser9} (Sup Fig 4 and 5 respectively). Our results showed that pSnpI^{Ser9} levels were similar in all three conditions. Furthermore, the marginal increase of pSnpI^{Ser9} levels at synaptic contacts in non-synchronised neurons treated with VPA was abolished in neurons pre-treated with Aβ42O (Sup Fig 4 D). This data suggests a possible antagonistic effect between Aβ42O and VPA.

Aβ42 oligomers affect the phosphorylation cycle of SnpI

Our results so far showed that exposure of neurons to Aβ42O results in sustained levels of pSnpI^{Ser9} at the pre-synaptic compartment of neurons recovering from depolarisation and that VPA attenuates this effect. We next examined if the increased levels of pSnpI^{Ser9} at synaptic contacts was due to restricted dispersal of pSnpI^{Ser9} or due to deregulation of the phosphorylation cycle of SnpI at Ser9. To do so, we examined the overall protein levels of both SnpI and pSnpI^{Ser9} for each condition by western blotting using protein extracts from neurons treated as previously described. We focused our analysis on protein extracts that were obtained from synchronised neurons and from neurons that recovered for 15 min after depolarisation (Fig 6).

First, we examined if treatment of neurons with either Aβ42O, VPA, or their combination (Aβ42O/VPA) affected the total amount of SnpI in depolarised hippocampal neurons. Western blots using antibodies for SnpI and actin (Act) were performed and the ratio of the signal intensity of SnpI over Act was calculated for all conditions and normalised against the SnpI/Act ratio of synchronised control neurons (marked as 100%). In addition, we also included co-treatment of Aβ42O with lower concentrations of VPA (1mM). Our results showed that in depolarised neurons (Fig 6 B black bars) and neurons allowed to recover for 15min (Fig 6B white bars), treatment with Aβ42O, VPA or both did not significantly alter the levels of SnpI.

Next, we examined the relative levels of pSnpI^{Ser9} under the same conditions (Fig 6C, D). Western blotting of protein extracts with antibodies for pSnpI^{Ser9} and SnpI was performed and the ratio of the signal intensity of pSnpI^{Ser9} over SnpI was calculated for all conditions. The pSnpI^{Ser9}/SnpI ratios were normalised to the ratio calculated from depolarised control neurons (marked as 100%). Comparison of the levels of pSnpI^{Ser9} after synchronisation for all treatments did not reveal any difference compared to control neurons (Fig 6D, black bars), suggesting that activity-dependent phosphorylation of SnpI at Ser9 remains unaffected by Aβ42O, VPA, or their combination. These results also suggest that the increase of pSnpI^{Ser9} at the presynaptic compartment in VPA treated neurons is not due to an increase in phosphorylation levels, but due to an increase in clustering of pSnpI^{Ser9}. However, differences were observed in neurons allowed to recover for 15 minutes after synchronisation (Fig 6D, white bars). Initially, we confirmed that the levels of pSnpI^{Ser9} were significantly reduced in recovering control neurons since this residue is believed to be dephosphorylated following neuronal activity (Fig 6D, $p<0.0001$ compared to control synchronised neurons). Although there was a reduction in the levels of pSnpI^{Ser9} in all conditions for recovering neurons relative to synchronised neurons (Fig 6D, $p<0.05$), there were significantly higher levels of pSnpI^{Ser9} in Aβ42O treated neurons compared to control neurons (Fig 6D, $p=0.015$). Interestingly, incubation with VPA restored the physiological cycle of SnpI dephosphorylation at Ser9 in a concentration-dependent manner ($p=0.045$ at 1mMVPA and $p=0.005$ at 10mM VPA compared to Aβ42O treated neurons).

These results confirm our previous observation and suggest that the elevated levels of pSnpI^{Ser9} at the presynapse of neurons exposed to Aβ42O is due to sustained levels of phosphorylated SnpI at position Ser9 rather than an increase in clustering of SnpI. Moreover, our data indicate that

the sustained levels of pSnpI^{Ser9} after depolarisation could be attenuated by a brief exposure of neurons (2hrs) to a near therapeutic dose of VPA (1mM), although a higher dose of 10mM was more effective.

Finally, to confirm that the deregulation of pSnpI^{Ser9} phosphorylation dynamics was specifically induced by Aβ42O, we repeated our experiments using an inverted Aβ peptide. Neurons were exposed to Aβ42O or to the inverted peptide and protein extracts from synchronised and recovered neurons were subjected to western blot analysis for SnpI and pSnpI^{Ser9} levels as previously described (Sup Fig 6). Our results showed that the elevated levels of pSnpI^{Ser9} in recovered neurons were only detectable in neurons exposed to Aβ42 and not in control neurons or in neurons exposed to the inverted Aβ peptide.

Aβ42 oligomers induce sustained phosphorylation of pSnpI^{Ser9}

Serine 9 in domain A of SnpI is phosphorylated by PKA and CaMKI/IV. Under basal conditions, low levels of constitutive phosphorylation are detected that rapidly increase following a depolarisation-induced Ca2+ influx (Czernik et al., 1987; Hosaka et al., 1999). The phosphate group on serine 9 is then removed by the phosphatase PP2A (Jovanovic et al., 2001). PP2A is a major serine/threonine phosphatase. It is a trimeric complex consisting of a core complex of a 65 kDa scaffolding subunit (A) and a 36 kDa catalytic subunit (C). The specificity and activity of PP2A is conferred when the core complex interacts with the B regulatory subunit. Phosphorylation of Tyr^{307} in the conserved C-terminus of the catalytic subunit inactivates PP2A (Chen et al., 1992). To examine sustained levels of pSnpI^{Ser9} in neurons exposed to Aβ42O were due to increased phosphorylation or decreased dephosphorylation activity on Ser9, we examined the relative phosphorylation levels of the catalytic subunits of PP2A$_C$ in extracts from neurons treated as previously described. Western blots using antibodies for Tyr^{307}-pPP2A$_{C\ \alpha/\beta}$ and actin (Act) were performed and the ratio of the intensity of Tyr^{307}-pPP2A$_C$ over Act was calculated for all conditions and subsequently normalised against the ratio of synchronised control neurons (marked as 100%). Our results showed that the phosphorylation levels of Tyr^{307}-pPP2A$_C$ were consistent in all conditions (Fig. 7). These results show that Aβ42O do not inactivate PP2A suggesting that the sustained levels of pSnpI^{Ser9} are due to sustained phosphorylation of Ser9.

Discussion

Aβ42O disrupt the regulation of SnpI

Extensive research has shown that synaptic dysfunction precedes the cognitive impairment in AD (Selkoe, 2002). However, the initial events underlying the early phases of this dysfunction are still not fully understood. Although there are several reports showing that intraneuronal accumulation of Aβ42 has a key role in early synaptic dysfunction (Gouras et al., 2010; Gouras et al., 2000; LaFerla et al., 2007; Oddo et al., 2006), the mechanisms are still obscure. Increasing evidence suggests that the aetiology of synaptic dysfunction in AD, might be linked to defects in the presynaptic bouton (Abramov et al., 2009; Parodi et al., 2010; Puzzo et al., 2008; Russell et al., 2012). Even though the cellular and molecular mechanisms are still poorly understood, these presynaptic defects have been associated with aberrant glutamate release promoting the activation of extrasynaptic neurotransmitter receptors, inducing the well-established excitotoxicity (Bordji et al., 2010; Li et al., 2011; Talantova et al., 2013), the inhibition of NMDAR-dependent LTP and a decrease in EPSPs (Walsh et al., 2002; Wang et al., 2002), the cellular and molecular mechanisms are still poorly understood.

To explore the mechanisms of neurotransmitter release affected by Aβ42O, we investigated if SnpI could be a target of Aβ42O. It has been shown in homogenates of post-mortem brains from individuals with confirmed AD, that SnpI was less susceptible to cAMP dependent phosphorylation *in vitro* on Ser9 due to higher basal phosphorylation levels in the diseased tissue (Parks et al., 1991). Considering this, we hypothesised that the dispersion of SnpI or its binding to SVs might be affected by Aβ42O. Comparing the extent of overlap between SnpI and Syp in neuronal cultures that were either non-synchronised, synchronised or were left to recover for 15min after synchronisation, we confirmed previous findings and showed in control neurons that activity dependent dispersion of SnpI from synaptic contacts was restored after 15min of recovery (Chi et al., 2001). We found no evidence that Aβ42O had a significant impact in this dispersion. Next, we examined if Aβ42O could affect the phosphorylation dynamics of $SnpI^{Ser9}$ that has been associated with binding to SVs. We confirmed previous findings and showed a transient increase of $pSnpI^{Ser9}$ at synaptic contacts of control depolarised neurons that was quickly restored in recovered neurons. Interestingly, in Aβ42O treated neurons recovering from depolarisation the presence of $pSnpI^{Ser9}$ at synaptic contacts was more pronounced compared to control. These results suggest that Aβ42O could alter the function of SnpI, either by preventing or delaying the dephosphorylation of $SnpI^{Ser9}$ after depolarisation, or by promoting clustering of $pSnpI^{Ser9}$ at synaptic contacts during the recovery period.

Having established the effects of Aβ42O in the regulation of SnpI, we then looked for available drugs that could antagonise this effect and identified VPA as a candidate molecule. VPA has been shown to induce clustering of SnpI (Hall et al., 2002) and also to prevent Aβ42O induced reduction in SV recycling (Williams and Bate, 2016). We confirmed previous reports suggesting that VPA can induce SnpI clustering (Hall et al., 2002) and showed that in mature neurons exposed to VPA the activity-dependent dispersion of SnpI from the synaptic bouton was reduced. Furthermore, VPA induced a minor increase of $pSnpI^{Ser9}$ at synaptic contacts in non-synchronised neurons, confirming a role of VPA in the activity dependent clustering of SnpI. In the presence of Aβ42O though, the minor presynaptic increase of $pSnpI^{Ser9}$ localisation induced by VPA was averted. Similarly, VPA inhibited Aβ42 from maintaining elevated levels of $pSnpI^{Ser9}$ at synaptic contacts after the recovery period, suggesting that VPA and Aβ42 oligomers might act antagonistically on the regulation of SnpI.

To demonstrate if the pre-synaptic increase of $pSnpI^{Ser9}$ was due to deregulation of the phosphorylation cycle of SnpI rather than clustering of $pSnpI^{Ser9}$, the relative protein levels of SnpI and $pSnpI^{Ser9}$ were analysed. Since the amount of $pSnpI^{Ser9}$ was increased in neurons exposed to Aβ42O and recovering from depolarisation, we concluded that the increased labelling of $pSnpI^{Ser9}$ at the presynapse was a result of an imbalance between dephosphorylation and/or sustained kinase activity on SnpI at Ser9 rather than a defect in clustering. Finally, since there weren't any differences in the phosphorylation levels of Tyr^{307} of the catalytic domain of PP2A we concluded that Aβ42O induced sustained kinase activity in depolarised hippocampal neurons.

Intracellular Aβ42: acute and chronic effects

It is important to understand how the data from our experiments relate to the synaptic dysfunction in early AD patients and to offer an explanation of available data regarding the effects of Aβ42 in NT release and SV availability (Abramov et al., 2009; Billings et al., 2005; Kelly and Ferreira, 2007; Oddo et al., 2003; Park et al., 2013; Parodi et al., 2010; Puzzo et al., 2008; Ripoli et al., 2013; Russell et al., 2012). Our data suggest that in neurons exposed to Aβ42O, the sustained phosphorylation levels of SnpI^{Ser9} after neuronal activity would prevent SnpI from stabilising SVs to the reserve pool after depolarisation, promoting an increase in their availability and consequently in glutamate release. This hypothesis would support several reports showing that Aβ42O affect glutamate release in a concentration and time dependent manner (Abramov et al., 2009; Parodi et al., 2010; Puzzo et al., 2008; Russell et al., 2012) and can be used to propose a mechanism to explain how the organisation of the SV pools is affected. For instance, Parodi et al. showed that exposure of neurons to low concentrations of Aβ provides a time dependent bell shaped effect in neurotransmitter release, with a significant increase during the first two hours of exposure followed by a substantial decrease below control levels after 24 hrs of exposure. What is more, the increased probability of release was associated with an increase of intracellular Ca^{2+} levels (Parodi et al., 2010). Our data fit well with this model since sustained intracellular Ca^{2+} levels would sustain CamKI/IV activity that would, in turn, maintain the increased levels of SnpI^{Ser9} we observed. Consequently, since increased SnpI^{Ser9} levels have been linked to an increased probability of NT release (Fiumara et al., 2004), the deregulation of the phosphorylation dynamics of SnpI can be a contributing factor to the aberrant glutamate release induced by Aβ42O during the initial exposure time. Furthermore, we have previously shown that Aβ42O disrupt the interaction between Syp and VAMP2 (Russell et al., 2012) at the presynapse. Syp regulates trafficking of VAMP2-containing SVs to the presynaptic bouton and upon stimulation the two proteins dissociate allowing VAMP2 to partake in the formation of the SNARE complex (Pennuto et al., 2003). Thus, the disruption of the Syp/VAMP2 complex by Aβ42O, would permit VAMP2 to participate in the formation of stable SNARE complexes. The increased probability of SNARE complex formation combined with an increased availability of SVs due to sustained pSnpI^{Ser9} levels could well be an additional contributing factor to the reported increase in the probability of glutamate release (Abramov et al., 2009; Parodi et al., 2010; Puzzo et al., 2008; Russell et al., 2012). In addition, it is likely that the disruption of the Syp/VAMP2 complex and the deregulation of SnpI would have a substantial additive impact in prolonged exposure to Aβ42O. Sustained phosphorylation levels of SnpI at Ser9, would prevent binding of SVs to the presynaptic actin cytoskeleton, allowing them to diffuse along the axon (Orenbuch et al., 2012). Inhibition of the Syp/VAMP2 complex formation by Aβ42O, would impede redistribution of the diffused SVs to the presynaptic terminal. This would contribute to the reported reduction of the size and regeneration of the SV pools (Bonanomi et al., 2007; Park et al., 2013; Parodi et al., 2010; Pennuto et al., 2003).

We also found evidence of a novel mode of action of VPA. VPA acts antagonistically to Aβ42O and prevents the deregulation of the phosphorylation dynamics of SnpI. Since this de-regulation is possibly an early event in the synaptic dysfunction induced by Aβ42O, we could hypothesise that early treatment with VPA would be more effective in antagonising these effects. Indeed, it has been shown that early application of the drug in a mouse model of AD was important to improve memory deficits (Qing et al., 2008). Whether VPA would be a suitable molecule to treat AD patients at later stages, depends on whether VPA interferes with molecular mechanisms associated with the later stages of AD which are yet to be characterised.

In conclusion, we believe that this study reveals a novel target of Aβ42 oligomers at the synapse, and highlights a mechanism that contributes to defective SV dynamics, which could contribute to the early synaptic dysfunction in AD. Importantly, we also provide an insight into a therapeutic role of VPA in protecting against Aβ42O -mediated synaptic deficits in AD. Collectively, these findings suggests a role for intraneuronal Aβ42O at the presynapse that could be a significant contributor to the onset and development of the disease. We believe this to be noteworthy since researching the effects of Aβ42 at the presynapse could help explain the progression of the disease, but will also enable identification of additional targets, essential for the development of efficient AD therapies.

Author contribution

JM: data collection and analysis, manuscript writing and revision. SHB: data collection. RW: manuscript revision. GD: manuscript revision and supervision. PA: conception and design, data analysis, manuscript writing and revision. This research did not receive any specific grant from funding agencies in the public, commercial, or not-for-profit sectors.

The authors declare no conflict of interest

Figure legends

Figure 1

Representative images of double immunolabeling for Syp (green) and SnpI (red) in control (A-C) and Aβ42O (300nM) treated primary hippocampal neurons (D-F) that were either non-synchronised (A, D), synchronised (B, E) or assayed 15min post synchronisation (C, F). High magnification of the boxed area is presented at the bottom of each picture. The extent of overlap between SnpI and Syp represented by the Mander's coefficient (G) showed an extensive overlap between the two proteins in non-synchronised neurons, that was temporarily reduced upon synchronisation and re-established after 15min of recovery in both, control and Aβ42O treated neurons (M=0.74±0.07, 0.34±0.06 and 0.63±0.16 in control and 0.73±0.09, 0.40±0.12 and 0.74±0.05 in Aβ42O treated neurons respectively). n=3 independent experiments. ***: p<0.0001. Scale bar, 10µm.

Figure 2

Representative images of double immunolabeling for Syp (green) and pSnpI^{Ser9} (red), in control (A-C) and Aβ42O (300nM) treated primary hippocampal neurons (D-F) that were either non-synchronised (A, D), synchronised (B, E) or assayed 15min post synchronisation (C, F). High magnification of the boxed area is presented at the bottom of each picture. The extent of overlap between Syp and pSnpI^{Ser9} represented by the Mander's coefficient (G) showed low levels of overlap between the two proteins in non-synchronised control and Aβ42O treated neurons, that was significantly increased upon synchronisation with M=0.19±0.07, 0.45±0.15 (p<0.0001, n=3) for control and 0.16±0.07, 0.52±0.19 (p<0.0001, n=3) for Aβ42O-treated neurons respectively. 15min post synchronisation, pSnpISer9 in control neurons was barely detectable (C) whereas in Aβ42O treated neurons a clear signal was evident (F). The extent of overlap between Syp and pSnpI^{Ser9}was severely reduced in control neurons compared to synchronised (M=0.06±0.02, p<0.0001, n=3). In Aβ42O-treated neurons, although the extent of overlap between Syp and pSnpI^{Ser9} was reduced compared to synchronised neurons (M=0.36±0.15, p= 0.048, n=5), it was significantly higher compared to control neurons (p<0.0001). ***: p<0.0001, *: p<0.05. Scale bar, 10µm.

Figure 3

Representative images of double immunolabeling for Syp (green) and SnpI (red), in control (A-C) and VPA (10mM) treated primary hippocampal neurons (D-F) that were either non-synchronised (A, D), synchronised (B, E) or assayed 15min post synchronisation (C, F). High magnification of the boxed area is presented at the bottom of each picture. The extent of overlap between SnpI and Syp represented by the Mander's coefficient (G) was similar between the two proteins in control and VPA treated non-synchronised neurons (M=0.74±0.07 and 0.69±0.04, n=3). In synchronised neurons an increase was evident in VPA treated neurons compared to control (M=0.35±0.06 and 0.48±0.06, respectively, p=0.03, n=3). In contrast, no difference was observed between control and VPA treated neurons 15min post synchronisation (M=0.64±0.05, 0.60±0.06). *: p<0.05. Scale bar, 10µm.

Figure 4

Representative images of double immunolabeling for Syp (green) and pSnpI^{Ser9} (red), in control (A-C) and VPA (10mM) treated primary hippocampal neurons (D-F) that were either non-synchronised (A, D), synchronised (B, E) or assayed 15min post synchronisation (C, F). High magnification of the boxed area is presented at the bottom of each picture. The extent of overlap between pSnpISer9 and Syp represented by the Mander's coefficient (G) in non-synchronised neurons, was slightly increased in VPA treated neurons (M=0.19±0.08 for control and 0.28±0.09 For VPA treated neurons, p=0.026, n=3), whereas it was similar in synchronised and in 15min post-synchronised control and VPA treated neurons (M=0.45±0.05, 0.05±0.02 for control and 0.39±0.06, 11±0.09 for VPA treated neurons respectively, n=3). *: p<0.05. Scale bar, 10µm.

Figure 5

Representative images of double immunolabeling for Syp (green) and pSnpI^{Ser9} (red), in control (A), Aβ42O (300nM) treated (B) and Aβ42O/VPA (300nM and 10mM respectively) treated neurons (C) that were assayed 15min post synchronisation. High magnification of the boxed area is presented at the bottom of each picture. The extent of overlap between Syp and pSnpI^{Ser9} represented by the Mander's coefficient (D) showed that the increase of pSnpI^{Ser9} at synaptic contacts induced by Aβ42O (0.36±0.15)

is reduced in the presence of VPA to similar levels as control neurons (0.09±0.02, and 0.06±0.02 respectively, n=3). ***: p<0.0001. Scale bar, 10µm.

Figure 6

Western blotting of protein extracts from mature primary hippocampal neurons for SnpI (A) and SnpIpSer9 (C). The intensity ratios of SnpI/Act (B) and $pSnpI^{Ser9}$/SnpI (D) were calculated for synchronised neurons (black bars) as well as for neurons 15min after depolarisation (white bars). All ratios were normalised to the SnpI/Act and $pSnpI^{Ser9}$/SnpI ratios of synchronised control neurons. No significant differences in the levels of SnpI were observed (p values >0.1, n=4). Quantification of the signal intensity of $pSnpI^{Ser9}$ over SnpI in synchronised neurons showed similar $pSnpI^{Ser9}$ levels in all conditions (D), whereas in recovered neurons, a substantial decrease of $pSnpI^{Ser9}$ levels was detected in control and VPA treated neurons (48.7%±11.9 in control, 42.5%±11.38 at 1mMVPA and 47.8%±12.57 at 10mM VPA, p<0.05 n=4) compared to synchronised neurons. However, in Aβ42O treated neurons, $pSnpI^{Ser9}$ levels remained elevated (74.07%±4.12, p=0.015 compared to control). After co-treatment with VPA, $pSnpI^{Ser9}$ levels were restored to control levels in a concentration dependent manner (40.13±14.15 with 10mM VPA, p=0.005 and 55.82±13.48, p=0.045 with 1mMVPA, n=4). **:p≤0.05, ***p<0.005.

Figure 7

Western blotting of protein extracts from mature primary hippocampal neurons for Tyr307-$pPP2A_{C\,\alpha/\beta}$ and Actin (A). The intensity ratios of Tyr307-$pPP2A_{C\,\alpha/\beta}$ /Act (B) were calculated and normalised to the Tyr307-$pPP2A_{C\,\alpha/\beta}$ /Act ratio of synchronised control neurons. No significant differences in the levels of Tyr307-$pPP2A_{C\,\alpha/\beta}$ were observed (p values >0.1, n=4).

References

Abramov, E., et al., 2009. Amyloid-beta as a positive endogenous regulator of release probability at hippocampal synapses. Nat Neurosci. 12**,** 1567-76.

Arias, C., et al., 1995. beta-Amyloid peptide fragment 25-35 potentiates the calcium-dependent release of excitatory amino acids from depolarized hippocampal slices. J Neurosci Res. 41**,** 561-6.

Benfenati, F., et al., 1989. Interactions of synapsin I with small synaptic vesicles: distinct sites in synapsin I bind to vesicle phospholipids and vesicle proteins. J Cell Biol. 108**,** 1863-72.

Benfenati, F., et al., 1992. Interaction of free and synaptic vesicle-bound synapsin I with F-actin. Neuron. 8**,** 377-86.

Benfenati, F., et al., 1991. Computer modeling of synapsin I binding to synaptic vesicles and F-actin: implications for regulation of neurotransmitter release. Proc Natl Acad Sci U S A. 88**,** 575-9.

Billings, L. M., et al., 2005. Intraneuronal Abeta causes the onset of early Alzheimer's disease-related cognitive deficits in transgenic mice. Neuron. 45**,** 675-88.

Bolte, S., Cordelieres, F. P., 2006. A guided tour into subcellular colocalization analysis in light microscopy. J Microsc. 224**,** 213-32.

Bonanomi, D., et al., 2007. Synaptophysin I selectively specifies the exocytic pathway of synaptobrevin 2/VAMP2. Biochem J. 404**,** 525-34.

Bordji, K., et al., 2010. Activation of extrasynaptic, but not synaptic, NMDA receptors modifies amyloid precursor protein expression pattern and increases amyloid-ss production. J Neurosci. 30**,** 15927-42.

Cesca, F., et al., 2010. The synapsins: key actors of synapse function and plasticity. Prog Neurobiol. 91**,** 313-48.

Chang, P., et al., 2010. Inhibition of long-term potentiation by valproic acid through modulation of cyclic AMP. Epilepsia. 51**,** 1533-42.

Chen, J., et al., 1992. Regulation of protein serine-threonine phosphatase type-2A by tyrosine phosphorylation. Science. 257**,** 1261-4.

Chi, P., et al., 2001. Synapsin dispersion and reclustering during synaptic activity. Nat Neurosci. 4**,** 1187-93.

Czernik, A. J., et al., 1987. Amino acid sequences surrounding the cAMP-dependent and calcium/calmodulin-dependent phosphorylation sites in rat and bovine synapsin I. Proc Natl Acad Sci U S A. 84**,** 7518-22.

Fiumara, F., et al., 2004. Phosphorylation by cAMP-dependent protein kinase is essential for synapsin-induced enhancement of neurotransmitter release in invertebrate neurons. J Cell Sci. 117**,** 5145-54.

Gouras, G. K., et al., 2010. Intraneuronal beta-amyloid accumulation and synapse pathology in Alzheimer's disease. Acta Neuropathol. 119**,** 523-41.

Gouras, G. K., et al., 2000. Intraneuronal Abeta42 accumulation in human brain. Am J Pathol. 156**,** 15-20.

Hall, A. C., et al., 2002. Valproate regulates GSK-3-mediated axonal remodeling and synapsin I clustering in developing neurons. Mol Cell Neurosci. 20**,** 257-70.

Harris, M. E., et al., 1995. beta-Amyloid peptide-derived, oxygen-dependent free radicals inhibit glutamate uptake in cultured astrocytes: implications for Alzheimer's disease. Neuroreport. 6**,** 1875-9.

Hosaka, M., et al., 1999. A phospho-switch controls the dynamic association of synapsins with synaptic vesicles. Neuron. 24**,** 377-87.

Hsia, A. Y., et al., 1999. Plaque-independent disruption of neural circuits in Alzheimer's disease mouse models. Proc Natl Acad Sci U S A. 96**,** 3228-33.

Hu, J. P., et al., 2011. Valproate reduces tau phosphorylation via cyclin-dependent kinase 5 and glycogen synthase kinase 3 signaling pathways. Brain Res Bull. 85**,** 194-200.

Jovanovic, J. N., et al., 2001. Opposing changes in phosphorylation of specific sites in synapsin I during Ca2+-dependent glutamate release in isolated nerve terminals. J Neurosci. 21**,** 7944-53.

Kabogo, D., et al., 2008. beta-Amyloid-related peptides potentiate K+-evoked glutamate release from adult rat hippocampal slices. Neurobiol Aging. 31**,** 1164-72.

Kelly, B. L., Ferreira, A., 2007. Beta-amyloid disrupted synaptic vesicle endocytosis in cultured hippocampal neurons. Neuroscience. 147**,** 60-70.

Lacor, P. N., et al., 2007. Abeta oligomer-induced aberrations in synapse composition, shape, and density provide a molecular basis for loss of connectivity in Alzheimer's disease. J Neurosci. 27**,** 796-807.

LaFerla, F. M., et al., 2007. Intracellular amyloid-beta in Alzheimer's disease. Nat Rev Neurosci. 8**,** 499-509.

Lambert, M. P., et al., 1998. Diffusible, nonfibrillar ligands derived from Abeta1-42 are potent central nervous system neurotoxins. Proc Natl Acad Sci U S A. 95**,** 6448-53.

Leng, Y., et al., 2008. Synergistic neuroprotective effects of lithium and valproic acid or other histone deacetylase inhibitors in neurons: roles of glycogen synthase kinase-3 inhibition. J Neurosci. 28**,** 2576-88.

Li, S., et al., 2009. Soluble oligomers of amyloid Beta protein facilitate hippocampal long-term depression by disrupting neuronal glutamate uptake. Neuron. 62**,** 788-801.

Li, S., et al., 2011. Soluble Aβ Oligomers Inhibit Long-Term Potentiation through a Mechanism Involving Excessive Activation of Extrasynaptic NR2B-Containing NMDA Receptors. J. Neuroscience. 31**,** 6627-6638.

Oddo, S., et al., 2003. Triple-transgenic model of Alzheimer's disease with plaques and tangles: intracellular Abeta and synaptic dysfunction. Neuron. 39**,** 409-21.

Oddo, S., et al., 2006. A dynamic relationship between intracellular and extracellular pools of Abeta. Am J Pathol. 168**,** 184-94.

Orenbuch, A., et al., 2012. Synapsin selectively controls the mobility of resting pool vesicles at hippocampal terminals. J Neurosci. 32**,** 3969-80.

Park, J., et al., 2013. Deleterious effects of soluble amyloid-beta oligomers on multiple steps of synaptic vesicle trafficking. Neurobiol Dis. 55**,** 129-39.

Park, J. H., et al., 2014. Effects of cerebrovascular disease and amyloid beta burden on cognition in subjects with subcortical vascular cognitive impairment. Neurobiol Aging. 35**,** 254-60.

Parks, K. M., et al., 1991. Reduced in vitro phosphorylation of synapsin I (site 1) in Alzheimer's disease postmortem tissues. Brain Res Mol Brain Res. 9**,** 125-34.

Parodi, J., et al., 2010. Beta-amyloid causes depletion of synaptic vesicles leading to neurotransmission failure. J Biol Chem. 285**,** 2506-14.

Pennuto, M., et al., 2003. Synaptophysin I controls the targeting of VAMP2/synaptobrevin II to synaptic vesicles. Mol Biol Cell. 14**,** 4909-19.

Puzzo, D., et al., 2008. Picomolar amyloid-beta positively modulates synaptic plasticity and memory in hippocampus. J Neurosci. 28**,** 14537-45.

Qing, H., et al., 2008. Valproic acid inhibits Abeta production, neuritic plaque formation, and behavioral deficits in Alzheimer's disease mouse models. J Exp Med. 205**,** 2781-9.

Ripoli, C., et al., 2014. Intracellular accumulation of amyloid-beta (Abeta) protein plays a major role in Abeta-induced alterations of glutamatergic synaptic transmission and plasticity. J Neurosci. 34**,** 12893-903.

Ripoli, C., et al., 2013. Effects of different amyloid beta-protein analogues on synaptic function. Neurobiol Aging. 34**,** 1032-44.

Russell, C. L., et al., 2012. Amyloid-beta acts as a regulator of neurotransmitter release disrupting the interaction between synaptophysin and VAMP2. PLoS One. 7**,** e43201.

Selkoe, D. J., 2002. Alzheimer's disease is a synaptic failure. Science. 298**,** 789-91.

Selkoe, D. J., 2012. Preventing Alzheimer's disease. Science. 337**,** 1488-92.

Semerdjieva, S., et al., 2013. Activation of EphA receptors mediates the recruitment of the adaptor protein Slap, contributing to the downregulation of N-methyl-D-aspartate receptors. Mol Cell Biol. 33**,** 1442-55.

Shankar, G. M., et al., 2007. Natural oligomers of the Alzheimer amyloid-beta protein induce reversible synapse loss by modulating an NMDA-type glutamate receptor-dependent signaling pathway. J Neurosci. 27**,** 2866-75.

Shrestha, B. R., et al., 2006. Amyloid beta peptide adversely affects spine number and motility in hippocampal neurons. Mol Cell Neurosci. 33**,** 274-82.

Shupliakov, O., et al., 2011. How synapsin I may cluster synaptic vesicles. Semin Cell Dev Biol. 22**,** 393-9.

Talantova, M., et al., 2013. Abeta induces astrocytic glutamate release, extrasynaptic NMDA receptor activation, and synaptic loss. Proc Natl Acad Sci U S A. 110**,** E2518-27.

Walsh, D. M., et al., 2002. Naturally secreted oligomers of amyloid beta protein potently inhibit hippocampal long-term potentiation in vivo. Nature. 416**,** 535-9.

Wang, H. W., et al., 2002. Soluble oligomers of beta amyloid (1-42) inhibit long-term potentiation but not long-term depression in rat dentate gyrus. Brain Res. 924**,** 133-40.

Williams, R. S., Bate, C., 2016. An in vitro model for synaptic loss in neurodegenerative diseases suggests a neuroprotective role for valproic acid via inhibition of cPLA2 dependent signalling. Neuropharmacology. 101**,** 566-75.

Zhang, M. M., et al., 2003. Effects of sodium valproate on synaptic plasticity in the CA1 region of rat hippocampus. Food Chem Toxicol. 41**,** 1617-23.

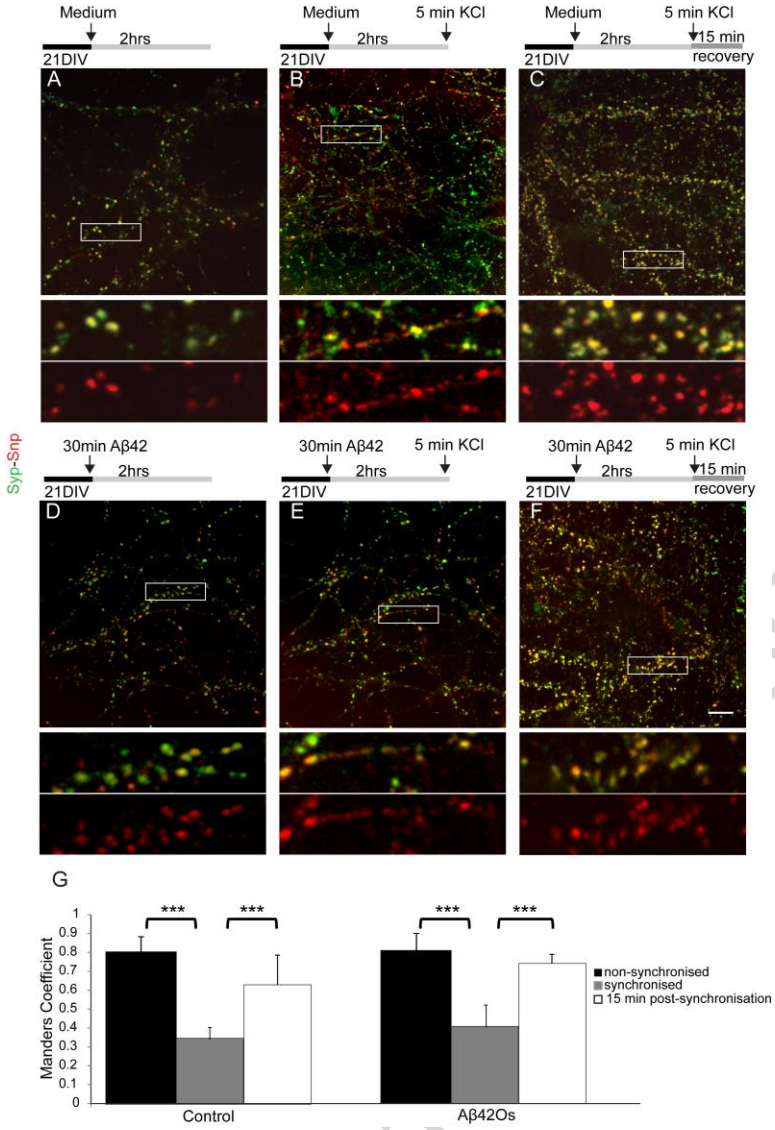

Fig. 1

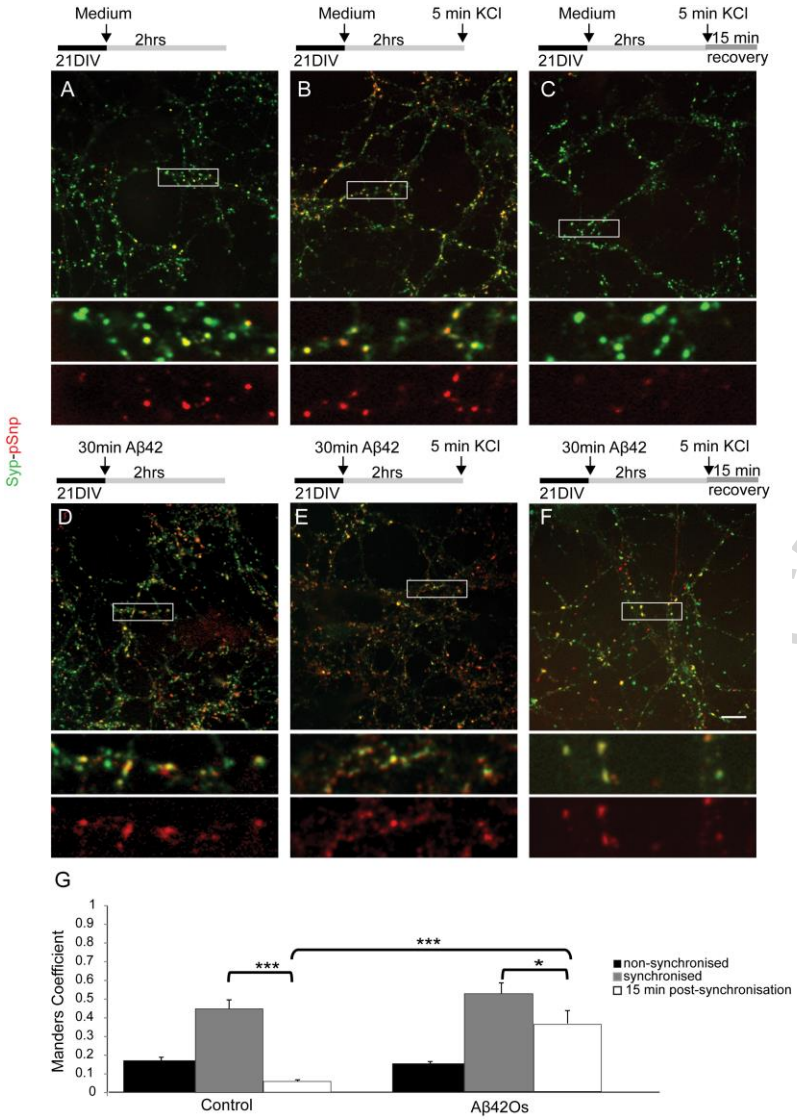

Fig. 2

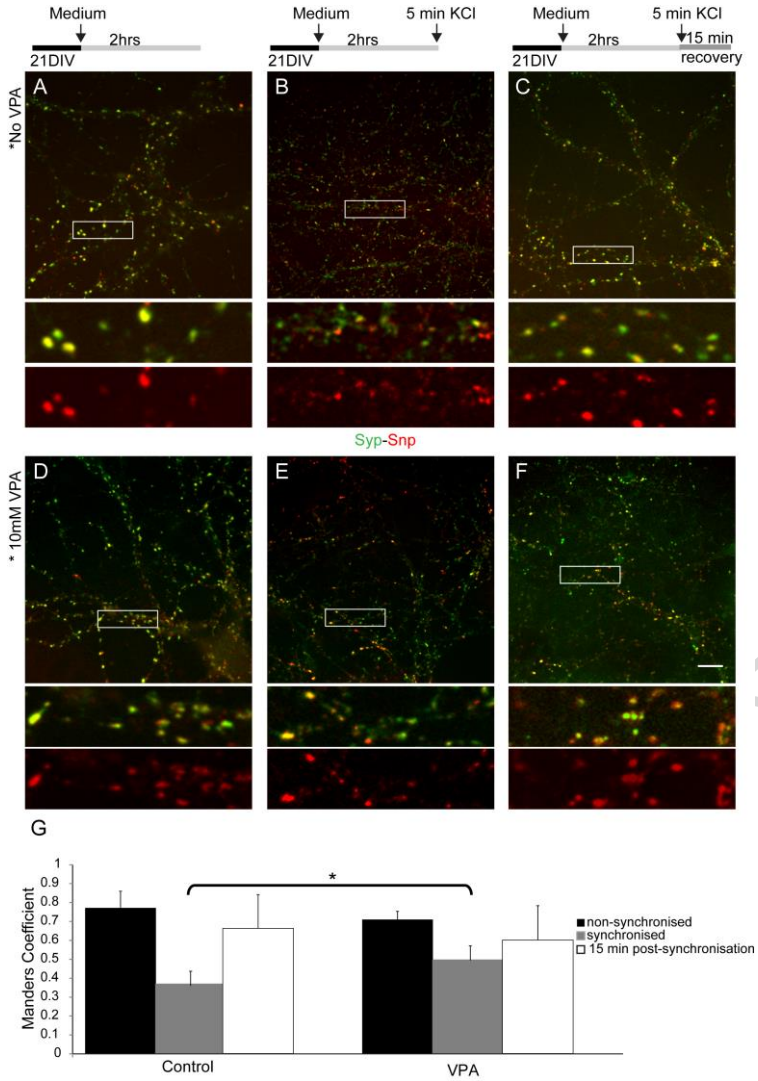

Fig. 3

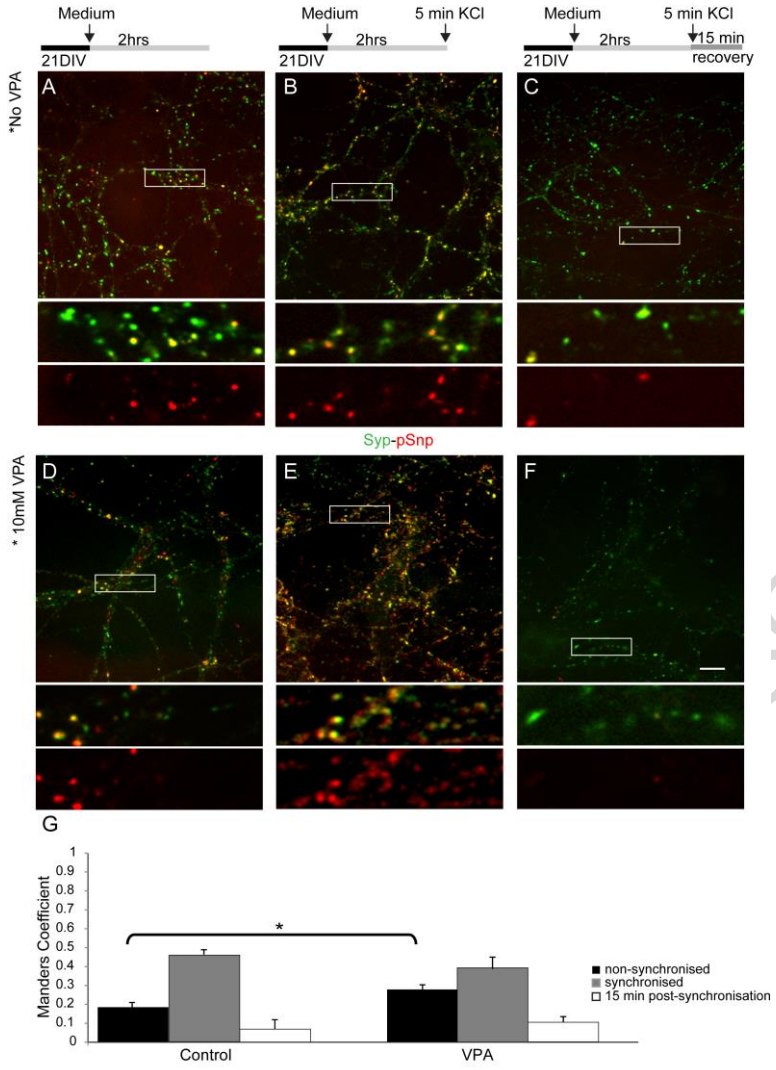

Fig. 4

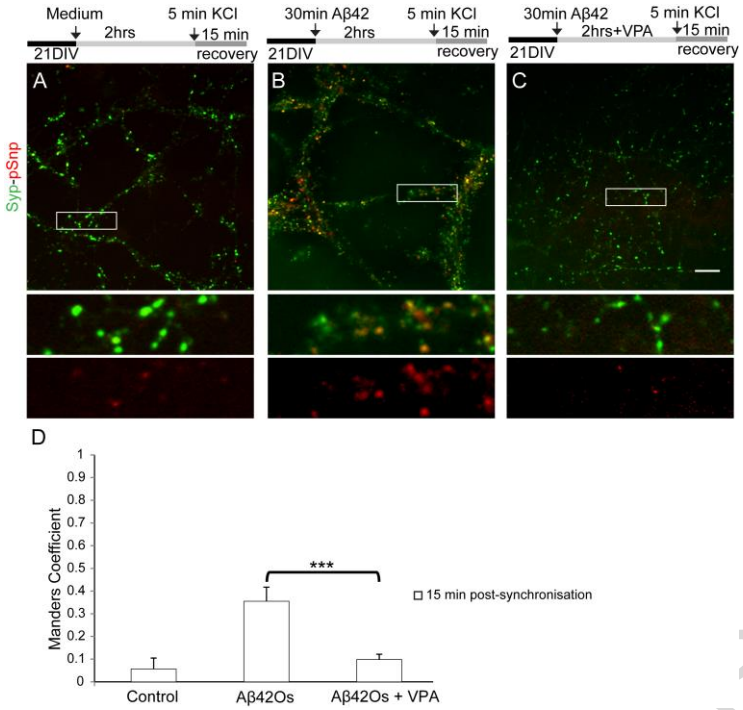

Fig. 5

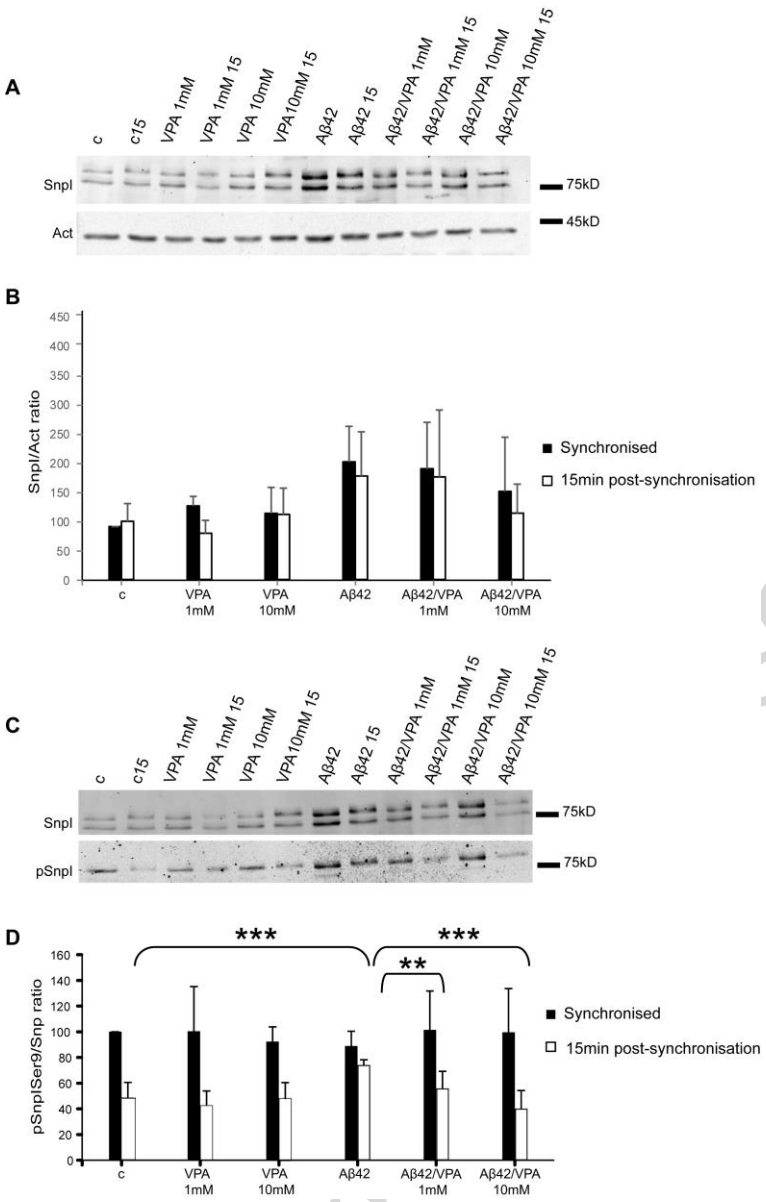

Fig. 6

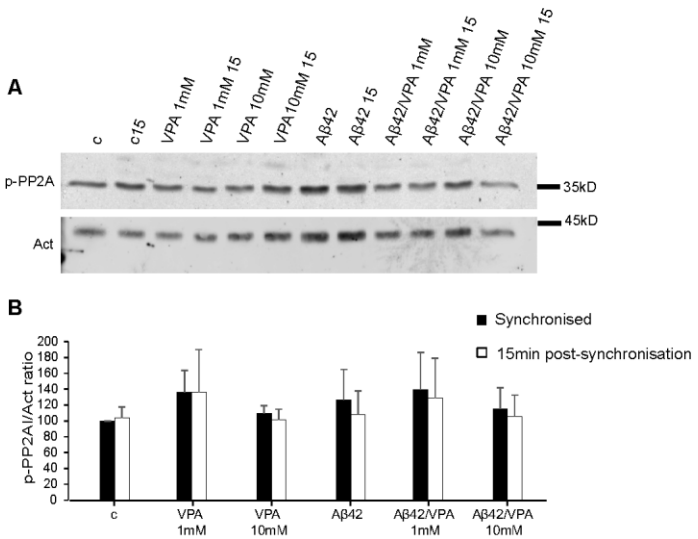

Fig. 7

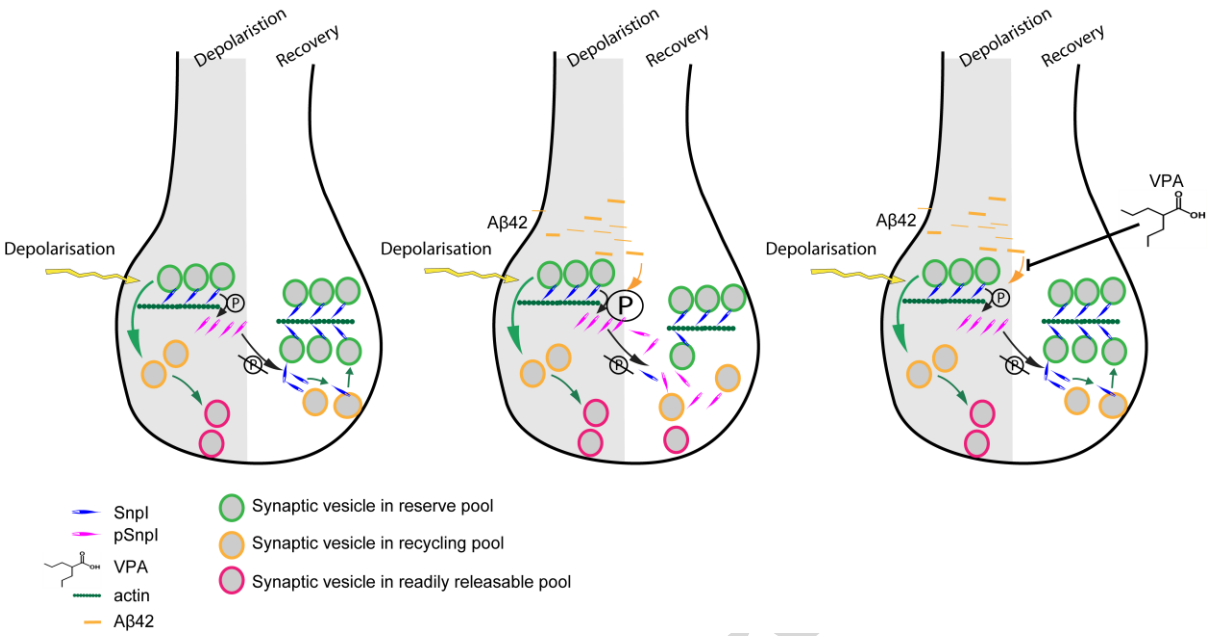

Graphical abstract

Highlights

- Activity dependent availability of synaptic vesicles is enhanced by Aβ42 oligomers
- Aβ42 oligomers reduce the recovery of SnpI after neuronal activity
- VPA reverses the effects of Aβ42 oligomers on SnpI